Journal of the Physical Society of Japan
Vol. 66, No. 11, November, 1997, pp. 3591-3599

Crossover from Vortex States to the Fulde-Ferrell-Larkin-Ovchinnikov State in Two-Dimensional s- and d-Wave Superconductors

Hiroshi SHIMAHARA* and Dierk RAINER[1]

Faculty of Integrated Arts and Sciences, Hiroshima University, Higashi-Hiroshima 739
[1]*Physikalisches Institut, Universität Bayreuth, D-95440 Bayreuth, Germany*

(Received April 17, 1997)

The effects of a tilted magnetic field on two-dimensional type-II superconductors of s- and d-wave pairing are studied. This includes a study of the crossover from vortex states to the Fulde-Ferrell-Larkin-Ovchinnikov (FFLO) state when the direction of the magnetic field is changed from perpendicular to the conducting plane to a parallel orientation. The FFLO state is obtained in the limit of a parallel magnetic field, and vortex phases with a large quantum number $n > 0$ (a higher Landau level) appear for tilted magnetic fields. At fixed tilt angle, the critical field exhibits a characteristic gtemperature dependence due to the change of the discrete quantum number. The relevance of the results for the observation and the identification of the FFLO state in the organic and high-T_c superconductors is discussed.

KEYWORDS: Fulde-Ferrell-Larkin-Ovchinnikov state, FFLO state, nonuniform superconductivity, two-dimensional superconductors, high-T_c superconductors, organic superconductors, upper critical field, vortex state

§1. Introduction

Fulde & Ferrell[1)] and independently Larkin & Ovchinnikov[2)] proposed in 1964 a new inhomogeneous superconducting state, which is considered the stable state at high magnetic fields in type-II superconductors with a strong Pauli paramagnetic effect. Compared to the traditional superconducting states this state is stabilized by a gain in spin-polarization energy. The observation of this state (FFLO state) requires clean type-II superconductors with a large critical field, such that pair breaking by the field acting on the spins (Chandrasekar-Clogston effect) is stronger than the usual orbital pair breaking which dominates in traditional type-II superconductors. A typical field which characterizes the amount of paramagnetic effects is the Pauli paramagnetic limit H_P. It is defined as the field at which the gain in spin-polarization energy in the normal state equals the superconducting condensation energy at $T = 0$ and $H = 0$. If an observed critical field exceeds the Pauli limit, the only presently available explanations would be triplet pairing, strong spin-orbit scattering, or a superconductor in the FFLO state. Hence, a superconductor with a critical field exceeding H_P is, in general, a possible candidate for finding the FFLO state. A direct verification of this state requires measuring the specific spatial variations of the order parameter predicted by FFLO.

Candidates for observing the FFLO state are heavy fermion superconductors, organic superconductors, and the layered copper oxide superconductors. These materials are clean type-II superconductors with a very high critical field. In fact, Gloos *et al.*[3)] have argued that the FFLO state was observed in the heavy fermion superconductor UPd_2Al_3, although until now there is no direct observation of the specific inhomogeneous structure of the FFLO state in this compound. In heavy fermion superconductors the orbital pairbreaking is strongly reduced by the very large effective mass (very low velocity) of the quasiparticle excitations, which leads to a very small orbital coupling and a very high critical magnetic field. The observed tricritical temperature[3)] of UPd_2Al_3 is much larger than the theoretical prediction so far, but can be explained by mixing of singlet and triplet order parameters, which is a natural consequence of the spatial oscillations and the Zeeman energy in FFLO superconductors.[4)]

Very high critical fields, which seem to exceed the Pauli paramagnetic limit, have been observed in some of the organic superconductors.[5-9)] A possible interpretation of these critical fields is in terms of the FFLO effect, although no direct evidence for the FFLO state has yet been reported. The origin of the high critical field of these systems lies in strong anisotropy of the conduction electron bands, which is a consequence of the layered crystal structure. A weak coupling of the layers leads to a very small electron velocity perpendicular to the conducting layers, and consequently to a very small orbital pairbreaking by magnetic fields oriented along the layers.

Our study in this paper is concerned with the organic and cuprate layered superconductors. These systems are good candidates for FFLO superconductivity, because (1) they are clean type-II superconductors, (2) the orbital effect can be strongly reduced by applying the magnetic field parallel to the conducting plane, and (3) Fermi surface effects are expected to enhance the critical field of the FFLO state remarkably in quasi-low-dimensional systems. The FFLO state in quasi-two-

* Present address: Faculty of Science, Hiroshima University, Higashi-Hiroshima 739.

dimensional (Q2D) compounds has been discussed by several authors. Early studies of the Q2D FFLO superconductor were published by Bulaevskii[10] and by Aoi *et al.*[11] They obtained the phase diagram on the H-T plane, which shows an enhanced critical field of the FFLO state, especially at low temperatures. Recently, Burkhardt and Rainer studied the FFLO state below the critical field and the lower critical field.[12] Shimahara[13,14] discussed the effects of Fermi surface structures on the FFLO state, and argued that Q2D organic superconductors including quasi-one-dimensional ones with sufficient curvature of the Fermi-surface to suppress the nesting instabilities are suited for observation of the FFLO state.

For ideally two-dimensional (2D) systems the orbital effect vanishes for magnetic fields pointing exactly along the conducting planes. For the more realistic Q2D systems one needs to take into account the following two points: Firstly, orbital effects may be important in real materials with an unavoidable finite inter-layer coupling, even for magnetic fields exactly parallel to the most conductive plane. Secondly, a magnetic field which is not perfectly oriented along the planes can lead to sizable orbital effects, even if the interplane coupling can be neglected. A nonzero perpendicular component of the magnetic field, even if it is very small, necessarily quantizes the in-plane orbital motion. This effect has serious consequences, because the structure of the in-plane vortex state competes with the structure of the FFLO state. Such a competition does not occur in three dimensional (3D) isotropic systems, where the order parameter can develop spatial FFLO oscillations in the direction of the magnetic field, whereas the orbital motion of the vortex state is perpendicular to the field.[15] Thus, the vortex state and the FFLO state can coexist in that case. The situation of layered superconductors with a negligible interlayer coupling was first studied by Bulaevskii.[10] He showed that a series of vortex states with higher Landau levels $n > 0$ appear because of the strong spin magnetic effect when the magnetic field is tilted away from perpendicular orientation. He also showed by numerical calculation that the critical field approaches that of the FFLO state when the parallel orientation is approached. Recent works on the combined effects of the spin and orbital magnetism are by Lebed',[16] Dupuis,[17] Yin and Maki,[18] Tachiki *et al.*,[19] and Maki and Won.[20] Lebed' calculated the FFLO critical field of Q1D superconductors in the presence of the orbital effect, and found that it is much higher than the conventional critical fields. Maki *et al.* also discussed the effect of interlayer motion of the electrons on the upper critical field of a layered superconductor as a model of the high-T_c superconductors. Matsuo *et al.*[21] and Shimahara *et al.*[22] studied the orbital magnetic effect in detail in d-wave type-II superconductors with crystal lattice anisotropy.

In this paper, we extend Bulaevskii's work on decoupled layers in a tilted field, and calculate the H-T phase diagram for finite tilt angles. We study superconductors which are strictly 2D apart from a very small interlayer coupling which suppresses fluctuations and stabilizes a BCS-like mean field superconductivity. In this sense, our system is a Q2D. We find characteristic features in the temperature dependence of the critical field due to changes of the discrete quantum number n of the vortex state. We also consider d-wave pairing, which is a widely accepted candidate for the pairing state in the organic and high-T_c superconductors, and we compare our result with that for s-wave pairing. The structure of the vortex lattice in a high-n state, and its crossover to the FFLO state will be discussed briefly.

In §2, we formulate the theory of the FFLO state for s- and d-wave pairing, including orbital effects. In §3, we show analytically how the order parameter and the critical field of FFLO state are recovered in the limit of a parallel magnetic field. It is analytically proved that the quantum numer n of the vortex state diverges in this limit, and an expression of n for small tilt angles is obtained. In §4, we present the phase diagrams in the H-T plane for various different tilt angles. The last section is devoted to the summary and discussion. In particular, we briefly analyse the perspectives for finding the FFLO state in organic and high-T_c superconductors.

§2. Formulation

We start with the linearized gap equation[10,15,21-25]

$$\Delta(\boldsymbol{r},\hat{\boldsymbol{p}}) = -\pi T \int_0^\infty \mathrm{d}t \frac{1-\mathrm{e}^{-\omega_D t}}{\sinh(\pi T t)} N(0) \int_0^{2\pi} \frac{\mathrm{d}\varphi'}{2\pi} V(\hat{\boldsymbol{p}},\hat{\boldsymbol{p}}') \cos[t\{h - \frac{1}{2}\boldsymbol{v}_F(\hat{\boldsymbol{p}}')\cdot\boldsymbol{\Pi}\}]\Delta(\boldsymbol{r},\hat{\boldsymbol{p}}'), \tag{2.1}$$

which includes the effect of the magnetic field on both the orbits and the spins. We have defined $h = \mu_0|\boldsymbol{H}|$ and $\boldsymbol{\Pi} = -\mathrm{i}\hbar\nabla - \frac{2e}{c}\boldsymbol{A}(\boldsymbol{r})$, with the electron magnetic moment $\mu_0 = -g\mu_B/2$, where $\mu_B = \hbar|e|/(2mc)$ and g are the Bohr magneton and the g-factor, respectively. $\boldsymbol{v}_F' = \boldsymbol{v}_F(\hat{\boldsymbol{p}}')$ is the Fermi-velocity, φ' is the angle between the momentum direction $\hat{\boldsymbol{p}}'$ and the p_x-axis, and $V(\hat{\boldsymbol{p}},\hat{\boldsymbol{p}}')$ is the interaction between two electrons with momenta $\boldsymbol{p}$ and $\boldsymbol{p}'$ on the Fermi surface, where $\hat{\boldsymbol{p}} = \boldsymbol{p}/|\boldsymbol{p}|$ and $\hat{\boldsymbol{p}}' = \boldsymbol{p}'/|\boldsymbol{p}'|$. The gap function is defined in the same way as in a previous paper.[22] We take units such that $\hbar = 1$.

We approximate the pairing interaction by $V(\hat{\boldsymbol{p}},\hat{\boldsymbol{p}}') = -g_\alpha\gamma_\alpha(\hat{\boldsymbol{p}})\gamma_\alpha(\hat{\boldsymbol{p}}')$, so that the gap function has the form $\Delta(\boldsymbol{r},\boldsymbol{p}) = \Delta_\alpha(\boldsymbol{r})\gamma_\alpha(\boldsymbol{p})$, and equation (2.1) can be written as

$$-\log(\frac{T}{T_c^{(0)}})\Delta_\alpha(\boldsymbol{r}) = \pi T \int_0^\infty \mathrm{d}t \frac{1}{\sinh(\pi T t)} \int_0^{2\pi} \frac{\mathrm{d}\varphi'}{2\pi} [\gamma_\alpha(\hat{\boldsymbol{p}}')]^2 [1 - \cos[t\{h - \frac{1}{2}\boldsymbol{v}_F'\cdot\boldsymbol{\Pi}\}]]\Delta_\alpha(\boldsymbol{r}), \tag{2.2}$$

where $T_c^{(0)} = 2e^{\gamma}\pi^{-1}\omega_D \exp(-1/g_\alpha N(0))$ is the zero field transition temperature with the Euler's constant $\gamma \approx 0.57721$.

In this paper, we assume a cylindrical Fermi surface and set the x- and y-axes in the conducting plane. The magnetic field lies in the yz plane,

$$\begin{aligned} \boldsymbol{H} &= (0, H_{/\!/}, H_\perp) \\ &= (0, H\cos\theta_H, H\sin\theta_H), \end{aligned} \tag{2.3}$$

and, with an appropriate gauge, the vector potential is given by

$$\begin{aligned} \boldsymbol{A} &= (A_x, 0, A_z) \\ &= (-H_\perp y, 0, -H_{/\!/} x). \end{aligned} \tag{2.4}$$

We define the differential operators, which satisfy bosonic commutation relations:

$$\begin{aligned} \eta_r &= \frac{1}{\sqrt{2\kappa_\perp}}(\Pi_x - \mathrm{i}\Pi_y) \\ \eta_r^\dagger &= \frac{1}{\sqrt{2\kappa_\perp}}(\Pi_x + \mathrm{i}\Pi_y) \end{aligned} \tag{2.5}$$

where $\kappa_\perp \equiv 2|e|H_\perp/c$. The parameter $\kappa_\perp$ expresses the strength of the orbital magnetic effect due to the tilted magnetic field. We should note here that η and $\eta^\dagger$ cannot be used for $\kappa_\perp = 0$. In terms of η and $\eta^\dagger$, the equation (2.2) is rewritten as

$$\begin{aligned} -\log\left(\frac{T}{T_c^{(0)}}\right)\Delta_\alpha(\boldsymbol{r}) = \pi T \int_0^\infty \mathrm{d}t \frac{1}{\sinh(\pi T t)} \int_0^{2\pi} \frac{\mathrm{d}\varphi'}{2\pi} [\gamma_\alpha(\hat{\boldsymbol{p}}')]^2 \\ \times \left[1 - \cos\left[ht - \frac{1}{2} t v_F \sqrt{\frac{\kappa_\perp}{2}} \{e^{\mathrm{i}\varphi'}\eta + e^{-\mathrm{i}\varphi'}\eta^\dagger\}\right]\right]\Delta_\alpha(\boldsymbol{r}). \end{aligned} \tag{2.6}$$

The second-order transition temperature and critical field are given by the solution of this equation with the minimum eigenvalue.

(i) s-wave case

First, we consider an s-wave pairing interaction, $[\gamma_s(\hat{\boldsymbol{p}})]^2 = 1$. In this case the integration over φ' in the gap equation (2.6) eliminates all terms with unequal powers in η and $\eta^\dagger$ (off-diagonal terms), and the eigenfunction of eq. (2.6) must be an eigenfunction of $\eta^\dagger\eta$. The Abrikosov functions

$$\phi_0^{(k)}(\boldsymbol{r}) = e^{\mathrm{i}kx} \exp\left[-\frac{\kappa_\perp}{2}\left(y - \frac{k}{\kappa_\perp}\right)^2\right] \tag{2.7}$$

satisfy the equation $\eta_r \phi_0^{(k)}(\boldsymbol{r}) = 0$ for any value of the parameter k. In addition, the boundary condition on $\Delta_\alpha(\boldsymbol{r})$ requires real k's. Hence, the eigenfunctions of $\eta^\dagger\eta$ belonging to an integer eigenvalue n are constructed from $\phi_0^{(k)}$ as

$$\phi_n^{(k)} = \frac{1}{\sqrt{n!}}(\eta^\dagger)^n \phi_0^{(k)}. \tag{2.8}$$

The suffix k is omitted in the following, because no mixing of $\phi_n^{(k)}$'s with different k occurs in eq. (2.6). Thus, for s-wave pairing the gap function must be proportional to one of the ϕ_n's. The critical field and temperature are given by

$$\begin{aligned} -\log\left(\frac{T}{T_c^{(0)}}\right) = \pi T \int_0^\infty \mathrm{d}t \frac{1}{\sinh(\pi T t)} \\ \times \left[1 - \cos(ht)\exp\left[\frac{-1}{16} t^2 {v_F}^2 \kappa_\perp\right] \sum_{k=0}^{n} \frac{(-1)^k n!}{k!^2 (n-k)!} \left[\frac{1}{8} t^2 {v_F}^2 \kappa_\perp\right]^k\right] \end{aligned} \tag{2.9}$$

with n optimized to give the largest H at fixed T and θ_H.

(ii) d-wave case

Next, we consider $d_{x^2-y^2}$-wave pairing interactions with $\gamma_d(\hat{\boldsymbol{p}}) = 2(\hat{p}_x^2 - \hat{p}_y^2)$, i.e., $[\gamma_d(\hat{\boldsymbol{p}})]^2 = 1 + \cos(4\varphi)$. In this case, the φ'-integral in eq. (2.6) produces off-diagonal terms of η and $\eta^\dagger$, because of the term $\cos(4\varphi)$ in $[\gamma_d(\hat{\boldsymbol{p}})]^2$. We expand the gap function in terms of the ϕ_n's as

$$\Delta_d(\boldsymbol{r}) = \sum_{n=0}^{\infty} \Delta_d^n \phi_n(\boldsymbol{r}), \tag{2.10}$$

and obtain the matrix equation

$$-\log\left(\frac{T}{T_c^{(0)}}\right)\Delta_d^n = \sum_{n'=0}^{\infty} D_{nn'}\Delta_d^{n'}, \tag{2.11}$$

with

$$D_{nn'} = \delta_{nn'} D_{nn} + (\delta_{n,n'+4} + \delta_{n+4,n'}) D_{nn'}^{(4)}, \tag{2.12}$$

where D_{nn} and $D_{nn'}^{(4)}$ are defined by

$$\begin{aligned} D_{nn} = \pi T \int_0^\infty \mathrm{d}t \frac{1}{\sinh(\pi T t)} \left[1 - \cos(ht)\exp\left[\frac{-1}{16} t^2 {v_F}^2 \kappa_\perp\right]\right. \\ \left. \times \sum_{k=0}^{n} \frac{(-1)^k n!}{k!^2 (n-k)!} \left[\frac{1}{8} t^2 {v_F}^2 \kappa_\perp\right]^k\right] \end{aligned} \tag{2.13}$$

$$D^{(4)}_{nn'} = -\frac{1}{2}\pi T \int_0^\infty \mathrm{d}t \frac{1}{\sinh(\pi T t)} \cos(ht) \exp[\frac{-1}{16} t^2 {v_\mathrm{F}}^2 \kappa_\perp] \times \sum_{k=0}^{\min(n,n')} \frac{(-1)^k \sqrt{n!n'!}}{k!(k+4)!(\min(n,n')-k)!} [\frac{1}{8} t^2 {v_\mathrm{F}}^2 \kappa_\perp]^{k+2}.$$

The resultant transition temperature $T = T_\mathrm{c}$ is given by the solution of eq. (2.11) with the mininum eigenvalue of the matrix $\hat{D} \equiv (D_{nn'})$. One can see from eq. (2.12) that Δ_d^n is mixed with $\Delta_d^{n\pm4}$ in eq. (2.11) for any n. Thus, the Δ_d^n's with $n = n_0, n_0+4, n_0+8, \cdots$ are all mixed, where n_0 can be equal to 0, 1, 2, and 3.

§3. Recovery of the FFLO State

In this section, we examine the gap equation in the limit of a parallel magnetic field and show that the FFLO state is recovered as the vortex state of infinite n. If we fix the quantum number n at any finite value, it is obvious that the critical field of the FFLO state is not recovered in the limit of the parallel magnetic field, i.e., $\kappa_\perp \to 0$. Taking the limit $\kappa_\perp \to 0$ with any fixed n in eq. (2.9) for s-wave pairing, and in eqs. (2.11), (2.12), and (2.13) for d-wave pairing, we obtain the equation for the transition point

$$-\log(\frac{T}{T_\mathrm{c}^{(0)}}) = \pi T \int_0^\infty \mathrm{d}t \frac{1}{\sinh(\pi T t)} [1 - \cos(ht)]. \quad (3.1)$$

This equation gives only the critical field of the traditional BCS state when the second-order transition is assumed.

On the other hand, if we consider the same model with an exactly parallel magnetic field ($\kappa_\perp = 0$), the critical field is determined by the appearance of the FFLO state. Replacing the gap function $\Delta_\alpha(\boldsymbol{r})$ with $\exp(\mathrm{i}\boldsymbol{q}\cdot\boldsymbol{r})$ in eq. (2.1), we obtain the equation for the FFLO critical field as

$$-\log(\frac{T}{T_\mathrm{c}^{(0)}}) = \pi T \int_0^\infty \mathrm{d}t \frac{1}{\sinh(\pi T t)} \int_0^{2\pi} \frac{\mathrm{d}\varphi}{2\pi} [\gamma_\alpha(\hat{\boldsymbol{p}})]^2 \times [1 - \cos[t\{h - \frac{1}{2}\boldsymbol{v}_\mathrm{F}\cdot\boldsymbol{q}\}]]. \quad (3.2)$$

The resultant critical field is obtained by optimizing $\boldsymbol{q}$.

The discrepancy between the critical field in the limit of $\kappa_\perp \to 0$ for any fixed finite n and that for $\kappa_\perp = 0$ leads to the result that the optimum quantum number n diverges when $\kappa_\perp \to 0$, unless the critical field and the gap function are singular at $\kappa_\perp = 0$ as functions of $\kappa_\perp$. We prove below that the FFLO critical field and the order parameter are recovered in this limit of n and $\kappa_\perp$. It is also shown that $q = |\boldsymbol{q}|$ of the FFLO state is expressed in this limit as

$$q = \lim_{\kappa_\perp \to 0} \sqrt{2\kappa_\perp n(\kappa_\perp)}, \quad (3.3)$$

where $n(\kappa_\perp)$ is the optimum n for each $\kappa_\perp$ and thus q is also optimized in the equation for $\kappa_\perp \to 0$.

It is plausible for the boson operator η to satisfy the equation

$$\eta^\dagger \phi_n \approx \sqrt{n} \mathrm{e}^{\mathrm{i}\varphi_0} \phi_n \quad (3.4)$$

for eigenfunctions of infinitly large n. From the expression (2.5) of η, this equation leads to the following two results. First, by solving eq. (3.4), we obtain

$$\phi_\infty \propto \exp(\mathrm{i}\boldsymbol{q}\cdot\boldsymbol{r}) \quad (3.5)$$

with $\boldsymbol{q} = (q\cos\varphi_0, q\sin\varphi_0, 0)$ and $q \equiv \lim_{\kappa_\perp\to0}\sqrt{2\kappa_\perp n}$. Secondly, $\eta^\dagger$ and η are replaced with $\sqrt{n}\mathrm{e}^{\mathrm{i}\varphi_0}$ and $\sqrt{n}\mathrm{e}^{-\mathrm{i}\varphi_0}$, respectively in the gap equation (2.6). Therefore, the FFLO critical field equation (3.2) is immediately recovered. Here, q is optimized so that the critical field is maximized, corresponding to the optimization of n. Therefore, if a solution with nonzero q is the optimum solution in the FFLO critical field equation, the optimized $n = n(\kappa_\perp)$ diverges as $n(\kappa_\perp) \approx q/\sqrt{2\kappa_\perp} \to \infty$ when $\kappa_\perp \to 0$.

Strictly speaking, a correct expression of eq. (3.4) is

$$(\eta^\dagger)^2 \phi_n \approx n \mathrm{e}^{2\mathrm{i}\varphi_0} \phi_n, \quad (3.6)$$

because $\eta^\dagger \phi_n \propto \phi_{n+1}$ and ϕ_n have different spatial symmetries. However, as is easily seen, eq. (3.4) and eq. (3.6) lead to the same result, when we use them in eq. (2.6). Then, eq. (3.5) is corrected as

$$\phi_\infty \propto \cos(\boldsymbol{q}\cdot\boldsymbol{r}) \quad \text{or} \quad \sin(\boldsymbol{q}\cdot\boldsymbol{r}). \quad (3.7)$$

For the s-wave pairing, since the gap function is proportional to one of ϕ_n's as we have seen in the previous section, it immediately follows that the spatial dependence of the FFLO gap function $\Delta_\alpha(\boldsymbol{r})$ is recovered in the limit of $n \to \infty$. This is confirmed also by the direct calculation of the gap function. The function $\phi_n^{(k)}(\boldsymbol{r})$ is expressed as

$$\phi_n^{(k)}(\boldsymbol{r}) = (-1)^n \mathrm{e}^{\mathrm{i}kx} H_n[\sqrt{2\kappa_\perp}(y - \frac{k}{\kappa_\perp})] \times \exp[-\frac{\kappa_\perp}{2}(y - \frac{k}{\kappa_\perp})^2] \quad (3.8)$$

in terms of the Hermite polynomial

$$H_n(x) \equiv (-1)^n \mathrm{e}^{x^2/2} \frac{\mathrm{d}^n}{\mathrm{d}x^n} \mathrm{e}^{-x^2/2} = \sum_{\substack{m=0 \\ (2m\le n)}} \frac{(-1)^m n!}{(n-2m)!\, 2^m m!} x^{n-2m}. \quad (3.9)$$

The behavior of the function $\phi_n^{(k=0)}$ for large n and small $\kappa_\perp$ with a fixed $q = \sqrt{2\kappa_\perp n}$ is easily examined for $y \ll \sqrt{2/\kappa_\perp}$. Since the terms with m such that $n - 2m$ is much smaller than n are dominant in the summation in eq. (3.9), we have

$$\phi_n^{(k=0)} \sim (-1)^{\frac{n}{2}} (\frac{n}{\mathrm{e}})^{\frac{n}{2}} \cos(qy) \quad (3.10)$$

for even n, and

$$\phi_n^{(k=0)} \sim (-1)^{\frac{n-1}{2}} (\frac{n}{\mathrm{e}})^{\frac{n}{2}} \sin(qy) \quad (3.11)$$

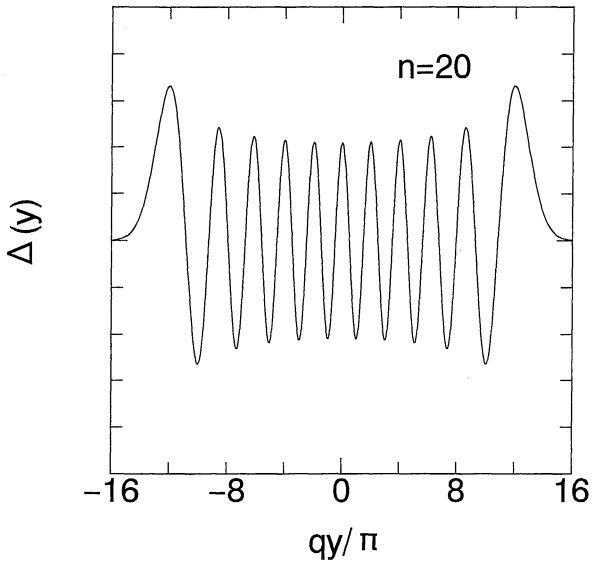

Fig. 1. The behavior of $\Delta(\boldsymbol{r}) \propto \phi_{20}^{(0)}$ calculated from eq. (3.8). The scale of the vertical axis varies with the magnetic field.

for odd n. Therefore, we obtain the FFLO order parameter in this limit. The behavior of $\Delta(\boldsymbol{r}) \propto \phi_n^{(k=0)}(\boldsymbol{r})$ with a large n is drawn in Fig. 1. It is localized and oscillates in space within a width several times $1/\sqrt{\kappa_\perp} \sim \sqrt{2n}/q$.

In eq. (3.10) and eq. (3.11), the spatial oscillation is in the direction along the y-axis, because we choose the solution with $k = 0$. The other directions of $\boldsymbol{q}$ are obtained by the gauge transformation

$$\boldsymbol{A} \to \tilde{\boldsymbol{A}} \equiv \boldsymbol{A} + \nabla\chi \tag{3.12}$$

with

$$\chi = H_\perp[\frac{1}{2}(x^2 - y^2)\sin\theta\cos\theta + xy\sin^2\theta], \tag{3.13}$$

where θ is the angle between the projection of $\tilde{\boldsymbol{A}}$ to the xy-plane and the x-axis. It is easy to see that the critical field and temperature are invariant under the gauge transformation as is expected.

For d-wave pairing it is difficult to calculate the $\kappa_\perp \to 0$ limit of the gap function directly from the expression (3.8) of ϕ_n, since an eigenfunction of the gap equation is a linear combination of ϕ_n's as in eq. (2.10). However, the eigenfunction with the minimum eigenvalue satisfies an equation of the same form as eq. (3.6) for $\kappa_\perp \to 0$, because the majority of the ϕ_n's in the linear combination must have infinitely large n. If ϕ_n with a finite n occupies a finite fraction of the linear combination of eq. (2.10), such a fraction reduces the critical field in the $\kappa_\perp \to 0$ limit, because such terms with finite n's converges to the uniform solution in that limit. Thus, linear combinations including terms of finite n's with finite amplitudes are not the eigenfunctions with the minimum eigenvalue, as far as the optimum solution of eq. (3.2) has a non-zero $\boldsymbol{q}$. Therefore, we can replace $\eta^\dagger$ and η with $\sqrt{n}e^{i\varphi_0}$ and $\sqrt{n}e^{-i\varphi_0}$, respectively, in eq. (2.6) in the limit of $\kappa_\perp \to 0$. In this equation, φ_0 is optimized as well as q, since the eigenvalues depend on φ_0 for d-wave pairing. Therefore, the FFLO gap function and critical field are recovered in the limit of $\kappa_\perp \to 0$. As in the s-wave case the physical results do not depend on the choice of the gauge. For the d-wave case, the expression eq. (2.13) is invariant except for additional phase factors $e^{\mp i4\theta}$ of $D^{(4)}_{nn'}$, which do not affect the eigenvalues.

§4. Phase Diagrams

As we have seen in §2, the critical field and temperature are determined by the first appearance of a high-n vortex state for magnetic fields not strictly parallel to the conducting plane. In this section, we examine the phase diagrams in the H-T plane for the s- and d-wave cases and for various tilt angles of the magnetic field.

First, we define the parameter r_m, which characterizes the strength of the orbital magnetic effect relative to that of the spin magnetic effect, as

$$r_m \equiv \frac{H_\perp}{z_m H} \tag{4.1}$$

with

$$z_m \equiv \frac{\dfrac{|h|}{2\pi T_c^{(0)}}}{\dfrac{2|e|}{c}(\dfrac{v_F}{2\pi T_c^{(0)}})^2 H} = \frac{\pi g}{4}\frac{T_c^{(0)}}{m{v_F}^2}. \tag{4.2}$$

We can take the three parameters, $T/T_c^{(0)}$, h/Δ_0, and r_m as the essential parameters in the gap equation, where $\Delta_0 = \pi/e^\gamma T_c^{(0)}$ is the zero field gap.

For small $\kappa_\perp$, the optimum $n = n(\kappa_\perp)$ is roughly estimated as a function of r_m as

$$n \sim \frac{|h|\bar{q}^2}{e^\gamma \Delta_0 r_m} \approx 0.561 \times \bar{q}^2 \frac{|h|}{\Delta_0}\cdot\frac{1}{r_m}, \tag{4.3}$$

with $\bar{q} \equiv v_F q/(2|h|)$, since $q \approx \sqrt{2\kappa_\perp n(\kappa_\perp)}$. For example, we have $n \sim 0.56/r_m$ at $T = 0$ in the s-wave case, because $\bar{q} = 1$ and $|h_c|/\Delta_0 = 1$ for the FFLO state when $r_m = 0$. Hence, for example for $r_m \sim 2$, the usual vortex state with $n = 0$ occurs at the critical field, while for $r_m \sim 0.5$, the vortex state with $n = 1$ occurs. Equation (4.3) results in that the optimum n increases when the temperature decreases, because $\bar{q}$ increases. For d-wave pairing, eq. (4.3) gives the value of n which mainly contributes to the optimum solution.

First, we examine the s-wave case. In this case, the tilt angle dependence of the critical field in the ground state was already obtained by Bulaevskii.[10] We study the ground state in more detail and, in addition, calculate the critical field for finite temperatures.

Figure 2 shows the result for $r_m = 0.5$. At each temperature the line with the highest critical field corresponds to the physical critical field. Thus, it is seen that the vortex state with $n = 1$ occurs at low temperatures in accordance with the above rough estimation, while the state with $n = 0$ occurs at high temperatures. One can see from this figure that the resultant critical field for $r_m = 0.5$ is already larger than the Pauli limit for $r_m = 0$.

The result for $r_m = 0.2$ is shown in Fig. 3. It is seen that vortex states with a higher n occur, and that the critical field of the ordinary FFLO state for parallel magnetic field is approached. The optimum value of the

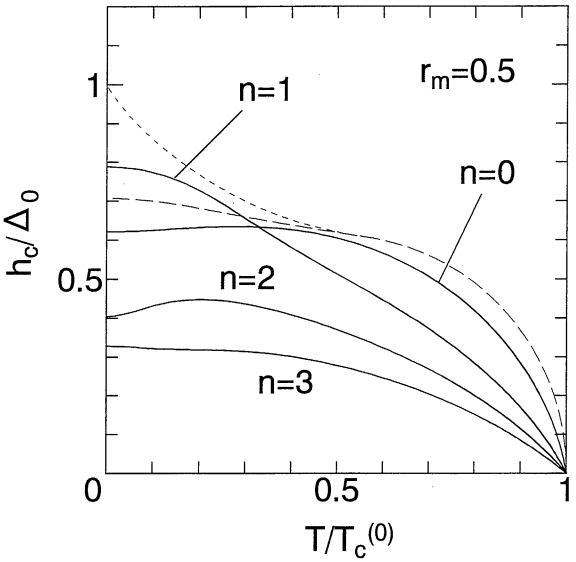

Fig. 2. The temperature dependence of the critical field for $r_m = 0.5$ in the s-wave case. The solid lines are the solutions of eq. (2.9) for fixed n. The physical critical field is the maximum one at each temperature. The broken and dotted lines show the Pauli paramagnetic limit of the BCS state with $q = 0$ and the critical field of the FFLO state, respectively, in the absence of the orbital effect, i.e., for $r_m = 0$.

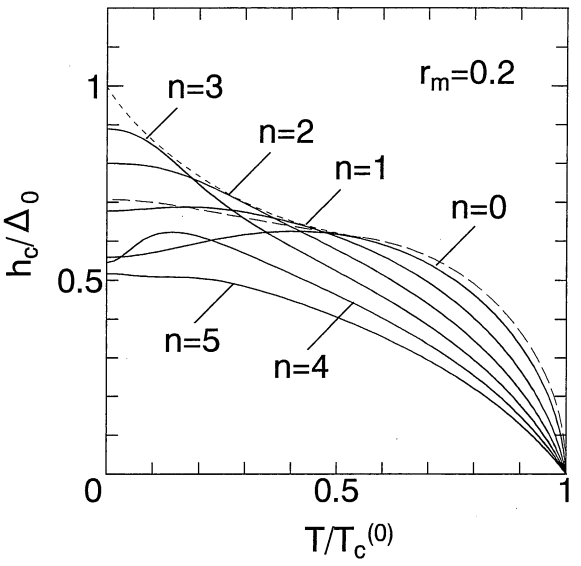

Fig. 3. The temperature dependence of the critical field for $r_m = 0.2$ in the s-wave case. The definitions of the solid, broken, and dotted lines are the same as in Fig. 2.

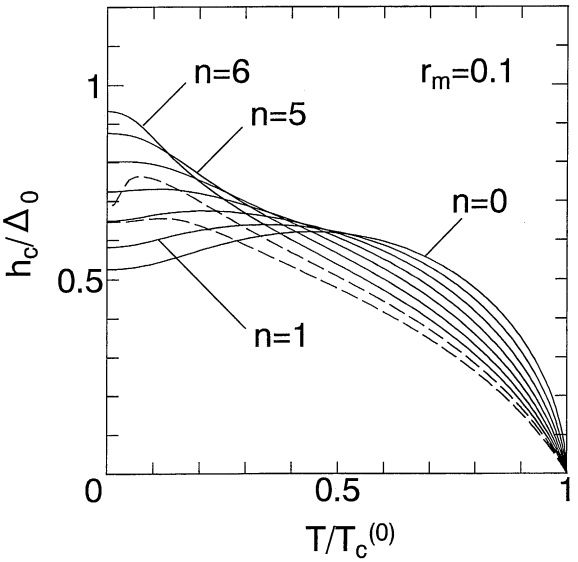

Fig. 4. The temperature dependence of the critical field for $r_m = 0.1$ in the s-wave case. The solid lines show the results for $n = 0, 1, 2, \cdots 6$, and the broken lines show the results for $n = 7$ and 8.

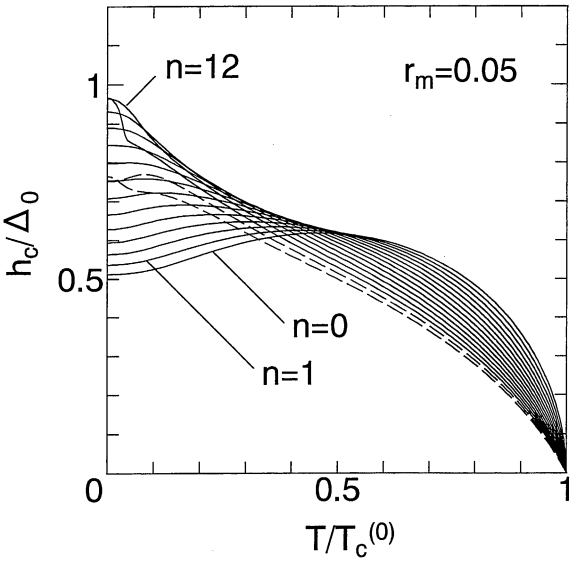

Fig. 5. The temperature dependence of the critical field for $r_m = 0.05$ in the s-wave case. The solid lines show the results for $n = 0, 1, 2, \cdots 13$, and the broken lines show the results for $n = 14$ and 15.

quantum number n of the vortex state at the critical field increases with decreasing temperature, as discussed above.

In these figures, we find a characteristic temperature dependence of the critical field due to the discrete change of the optimum n. The temperature derivative of the critical field shows jumps when n changes.

Figure 4 shows the result for $r_m = 0.1$. The optimum quantum number $n = 6$ at $T = 0$ coincides with the rough estimate given in eq. (4.3). The critical field curve becomes nearly smooth in spite of the discrete changes of n from $n = 0$ to $n = 6$. The results for a smaller r_m are depicted in Fig. 5. It is found that for $T/T_c^{(0)} \gtrsim 0.05$, the value $r_m = 0.05$ is sufficiently small so that the critical field h_c is indistinguishable from the FFLO critical field within the width of the lines. However, they differ for low temperatures $T/T_c^{(0)} \lesssim 0.05$. In particular, the linear temperature dependence of the FFLO critical field near $T = 0$ is not recovered even for $r_m = 0.05$.

The r_m dependence of the critical field at $T = 0$ is drawn in Fig. 6. The curves for $n = 1 \sim 6$ were already obtained by Bulaevskii,[10] except for a discrepancy in the scale of the r_m axis. The figure shows, in addition, the critical fields for larger n and smaller r_m, and it confirms

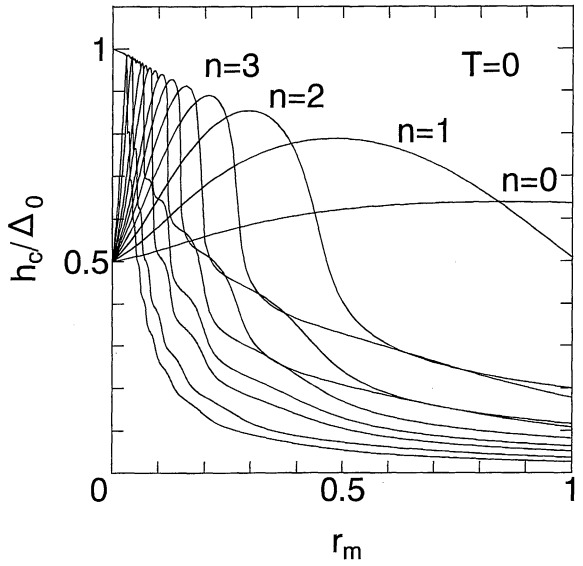

Fig. 6. The r_m dependence of the critical field at $T = 0$ in the s-wave case. The whole curves at fixed n are drawn for $n = 0$, 1, 2, 3, 4, 5, 6, 8, 10, 15, and 20.

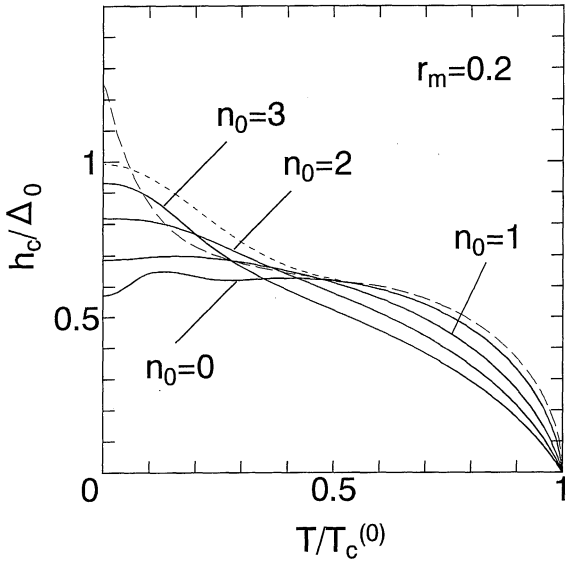

Fig. 8. The temperature dependence of the critical field for $r_m = 0.2$ in the d-wave case. The definitions of the solid, broken, and dotted lines are the same as Fig. 7.

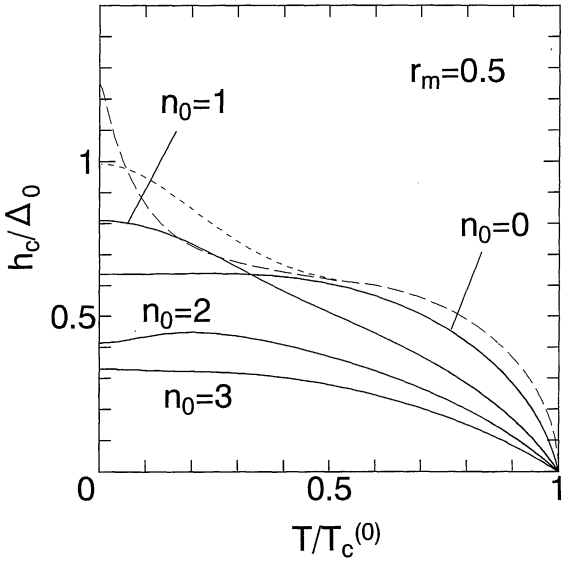

Fig. 7. The temperature dependence of the critical field for $r_m = 0.5$ in the d-wave case. The solid lines are the solutions of eq. (2.11) with fixed n_0. The physical critical field is the maximum one at each temperature. The broken and dotted lines show the critical field at $r_m = 0$, for $\varphi_{\boldsymbol{q}} = 0$ and $\pi/4$, respectively.

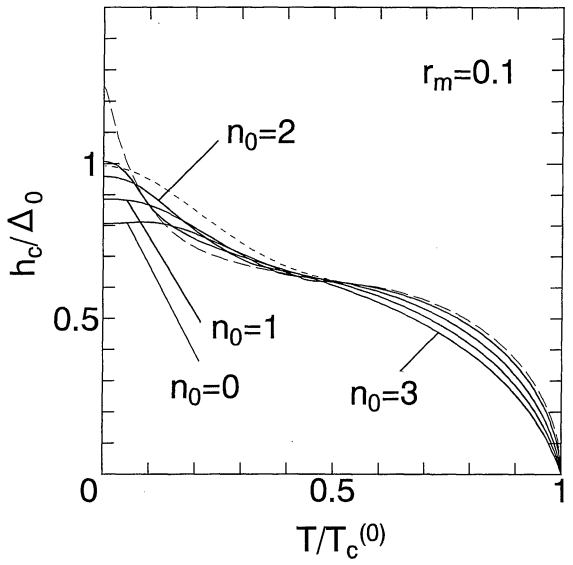

Fig. 9. The temperature dependence of the critical field for $r_m = 0.1$ in the d-wave case. The definitions of the solid, broken, and dotted lines are the same as Fig. 7.

numerically the recovery of the FFLO critical field in the limit of $r_m \to 0$. In this figure, the multipeak structure of the critical field obtained by Bulaevskii is seen. It is also found that the critical fields for $r_m \lesssim 0.74$ are larger than the Pauli paramagnetic limit $h_c = \Delta_0/\sqrt{2}$ for $r_m = 0$, and vortex states with a large quantum number $n \geq 1$ occur for $r_m \lesssim 0.84$.

Next, we consider the d-wave case. In this case, mixing between n and $n \pm 4$ occurs in the linearized gap equation, as we discussed in §2. The solutions are classified by n_0, which is the smallest value of n in each solution. When we solve the linearized gap equation (2.11) numerically, we need to set a sufficiently large cutoff n_c in the summation over n. We set the cutoff $n_c = n_0 + 4l_c$ with $l_c = 5$, which gives sufficiently accurate results for the parameters that we used in this paper. The results for the d-wave FFLO state at $r_m = 0$ were published by Maki *et al.*[20]

In Fig. 7, the temperature dependence of the critical field is shown for $r_m = 0.5$. As in the s-wave case, we already have a higher critical field for this large value of r_m than the Pauli paramagnetic limit. Fig. 8 shows the result for $r_m = 0.2$. The FFLO critical field with the optimum $\boldsymbol{q}$ is approached, as r_m becomes smaller. We find a characteristic temperature dependence due to the change of the optimum quantum number n_0 similar to that of the s-wave case. The mixing of n and $n \pm 4$ due to the anisotropy of the d-wave order parameter does not

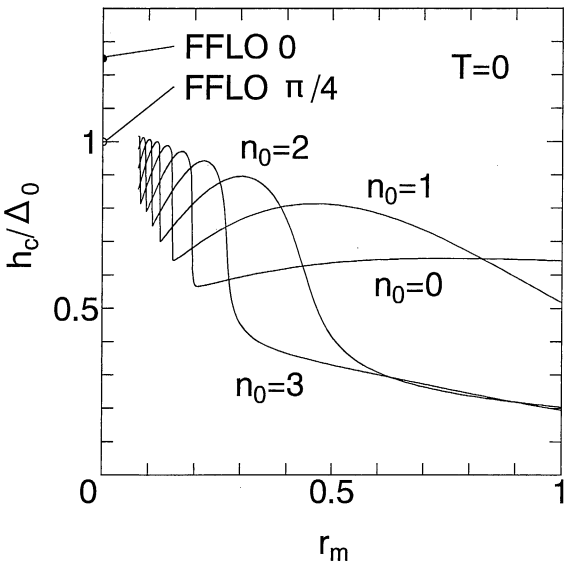

Fig. 10. The r_m dependence of the critical field at $T = 0$ in the d-wave case. The open and closed circles show the critical field of the FFLO state with $\varphi_{\boldsymbol{q}} = \pi/4$ and 0, respectively.

smear the discrete changes of the temperature derivative of the critical field.

Figure 9 shows the result for $r_m = 0.1$. Differently from the s-wave case the critical field is much smaller than that for $r_m = 0$, although the behavior is nearly smooth. Such slow convergence with respect to r_m is due to the mixing of n caused by the anisotropy of the d-wave order parameter. In particular, it is found that the rapid rise of the critical field of the FFLO state with $\varphi_{\boldsymbol{q}} = 0$ at low temperatures is not recovered, unless r_m is much smaller than 0.1, where $\varphi_{\boldsymbol{q}}$ is the angle between $\boldsymbol{q}$ and the p_x-axis.

The critical field at zero temperature is shown in Fig. 10. The results for small $r_m \lesssim 0.07$ are not shown because they are beyond our numerical accuracies. In this figure, we find the multipeak structure and the discrete behavior like for s-wave pairing, in spite of the mixing of n's. It is found that the vortex states with nonzero n essentially occur for $r_m \lesssim 0.83$.

§5. Summary and Discussion

We have studied the combined influence of spin and orbital magnetic effects on the critical fields of 2D type-II superconductors in a tilted magnetic field. When the tilt angle is small, i.e. when the magnetic field is nearly parallel to the conducting plane, the spin magnetic effect stabilizes vortex states of higher Landau levels, as first discussed by Bulaevskii for s-wave superconductors.[10] In this paper, we presented our calculations of the temperature dependence of the critical field at various tilt angles for s-wave and d-wave pairings, the latter of which is a widely accepted candidate for the type of pairing in organic and high-T_c superconductors. These calculations shall clarify the cross-over from the traditional vortex state at perpendicular field to the FFLO state at parallel field. We have examined the parallel field limit in detail, and have proved analytically that the FFLO state is recovered as a limit of the vortex state.

When the direction of the magnetic field changes from parallel to perpendicular to the conducting planes, the ratio r_m, defined by eq. (4.1), increases from zero to a very large value ($r_m = {z_m}^{-1}$). For the parallel magnetic field ($r_m = 0$) the spin effect favors the FFLO state, while for the non-parallel magnetic fields ($r_m \neq 0$) the orbital effect favors vortex states, because the orbital motions of the electrons are necessarily quantized for any nonzero r_m. The apparent incompatibility of the structures of the FFLO state at $r_m = 0$ and the vortex states for $r_m > 0$ is resolved in the following way. The FFLO state is exactly recovered as the $n \to \infty$ limit of the vortex states. At temperatures where the FFLO state exists for fields parallel to the planes ($r_m = 0$), the quantum number n of the optimum vortex state increases when r_m decreases. At other temperatures, the vortex state with $n = 0$ remains favored at arbitrary r_m. The relation of the three quantities n, r_m, and q is given by eq. (4.3) for small r_m's, where n is the optimum quantum number and q the wave vector of the stable FFLO state in the limit $r_m = 0$.

To illustrate that a strong spin effect results in the appearance of vortex states with non-zero n, we discuss the coefficient of the expansion of the gap equation in powers of $\kappa_\perp = 2|e|H_\perp/c$. Expansion of eq. (2.9) to the first order in $\kappa_\perp$ leads to

$$-\log\left(\frac{T}{T_c^{(0)}}\right) = \frac{{v_F}^2\kappa_\perp}{8(\pi T)^2}F\left(\frac{h}{\pi T}\right)\left(n+\frac{1}{2}\right), \tag{5.1}$$

where the function $F(a)$ is defined by

$$F(a) = \int_0^\infty du\, \cos(au)\frac{u^2}{\sinh(u)}. \tag{5.2}$$

This definition implies $F(a) > 0$ for $a < a_0 \approx 0.608$, while $F(a) < 0$ for $a > a_0$. Therefore, for weak spin magnetic effects such that $h/\pi T < a_0$, the coefficient of n is positive on the right hand side of eq. (5.1), and $n = 0$ is the optimum quantum number. On the other hand, for strong spin magnetic effect such that $h/\pi T > a_0$, the coefficient becomes negative, the lowest order expansion breaks down, and the vortex state with $n = 0$ is no longer the optimum solution.

The most remarkable feature of the H-T phase diagrams is the rugged behavior of the critical field. The slope of the critical field curve changes discontinuously at the temperatures where the optimum n changes. This behavior occurs also in the d-wave case. In spite of the mixing of the vortex states with n and $n \pm 4$, the rugged behaviors of the critical field as a function of temperature and the tile angle are not smeared. The calculated phase diagrams show, in accordance with eq. (3.3), that the optimum quantum number n increases with the decreasing temperature, since $\bar{q} \equiv v_F q/(2h_c)$ of the FFLO state increases. When r_m becomes smaller, the temperature dependence of the critical field becomes smoother. The rugged behaviors of the critical field as a function of temperature and tilt angle are helpful for an experimental identification of the high n vortex state. In particular, it would be easier to control the temperature for a fixed tilt angle than to control the tilt angle in a very narrow region of the order of z_m.

The critical field curve becomes nearly smooth at $r_m \lesssim 0.05 \sim 0.1$, and especially for s-wave case it becomes very close to the curve of the FFLO crtical field. However, for low temperatures, the convergence to the FFLO critical field is slow, and the typical linear temperature dependence of the FFLO critical field near $T = 0$ in 2D systems is not recovered even for a small $r_m = 0.05 \sim 0.1$, both in the s- and d-wave cases. For d-wave pairing, Maki *et al.*[20] argued that the appearance of the FFLO state is signaled by a rapid rise of the critical field at low temperatures, when the magnetic field is applied in the conducting plane. The slope of the FFLO critical field becomes very steep when the direction of $\boldsymbol{q}$ changes from $\varphi_{\boldsymbol{q}} = \pi/4$ to $\varphi_{\boldsymbol{q}} = 0$ discretely. However, depending on the material under consideration, such behavior is not recovered unless the magnetic field is applied accurately in the direction parallel to the conducting plane so that r_m becomes less than a value of the order of 0.1.

Now, we briefly discuss the organic and high-T_c superconductors. The parameter z_m defined by eq. (4.2) is expressed in terms of the effective mass $m^* = p_F/v_F$, the Fermi momentum p_F, and the BCS coherence length $\xi_0 \equiv v_F/(\pi\Delta_0)$ as

$$z_m = \frac{g}{4}\frac{T_c^{(0)}}{\Delta_0}\frac{m^*}{m}\frac{1}{p_F\xi_0} , \tag{5.3}$$

where $T_c^{(0)}/\Delta_0 = e^\gamma/\pi$ in the present weak coupling theory. For Q2D organic superconductors, if we assume $\xi_0 \sim 100$ Å, a lattice constant $a \sim 10$ Å, $m^* \sim 3m$, and $g \sim 2$, as an example, and estimate p_F by an equation p_F by $\pi {p_F}^2/(2\pi/a)^2 \sim 1/4$ for quarter filling, then we have $z_m \sim 1/20$ as a rough estimate. Therefore, for r_m to be of the order of 0.1 and 0.8 the tilt angle θ_H must be of the order of 0.3(deg) and 2.3(deg), respectively. We should note that these estimates are very crude, because we have ignored the interplane electron transfers, and assumed a simplified form of the pairing interactions and weak coupling theory.

On the other hand, for high-T_c superconductors, if we assume $\xi_0 \sim 20$ Å, $a \sim 4$ Å, $m^* \sim 2m$, and $g \sim 2$, $\pi {p_F}^2/(4\pi^2/a^2) \sim 0.5$ for nearly half-filling, as an example, then we estimate $z_m \sim 0.3$. Thus, for r_m to be of the order of 0.1 and 0.8, θ_H must be of the order of 1.7(deg) and 13.9(deg), respectively. Therefore, for the rapid rise due to d-wave pairing[20] to appear, the magnetic field has to be nearly parallel to the conducting plane so that $\theta_H \ll 1.7$(deg), while for the rugged behavior of the critical field to be observed, one needs $\theta_H \lesssim 13.9$(deg). If we take into account that the ratio $\Delta_0/T_c^{(0)}$ is a few times π/e^γ in the high-T_c superconductors, the estimated angles are modified to a few times smaller values. For comparison of the theory and experiments, the interplane transfers of holes are also important at moderate magnetic fields, while they are suppressed in the limit of high magnetic fields, according to Lebed's arguement.[16]

As a future study, the vortex lattice structure is relevant for the experimental identification of the high-n vortex states and the FFLO state in the Q2D system, by the scanning tunneling microscope (STM) technique. Small interplane electron transfers and the Fermi surface anisotropy, which are inevitable in the real materials, are also important subjects to study.

Acknowledgements

We would like to thank Prof. Ulf Klein, Dr. Hubert Burkhardt, Dr. Matthias Eschrig for useful discussions.

1) P. Fulde and R. A. Ferrell: Phys. Rev. **135** (1964) A550.
2) A. I. Larkin and Yu. N. Ovchinnikov: Zh. Eksp. Teor. Fiz. **47** (1964) 1136; translation: Sov. Phys. JETP **20** (1965) 762.
3) K. Gloos, R. Modler, H. Schimanski, C. D. Bredl, C. Geibel, F. Steglich, A. I. Buzdin, N. Sato and T. Komatsubara: Phys. Rev. Lett. **70** (1993) 501; H. Schimanski, K. Gloos, F. Martin, R. Modler, C. Geibel, C. Schank and F. Steglich: Physica B **199&200** (1994) 125.
4) S. Matsuo, H. Shimahara and K. Nagai: J. Phys. Soc. Jpn. **63** (1994) 2499.
5) K. Murata, M. Tokumoto, H. Bando, H. Tanino, H. Anzai, N. Kinoshita, K. Kajimura, G. Saito and T. Ishiguro: Physica B&C **135BC** (1985) 515.
6) K. Murata, N. Toyota, M. Tokumoto, H. Anzai, G. Saito, K. Kajimura, S. Morita, Y. Muto and T. Ishiguro: Physica B&C **143BC** (1986) 366.
7) K. Murata, Y. Honda, H. Anzai, M. Tokumoto, K. Takahashi, N. Kinoshita, T. Ishiguro, N. Toyota, T. Sasaki and Y. Muto: Synth. Met. **27** (1988) 341.
8) E. B. Yagubskii, I. F. Shchegolev, S. I. Pesotskii, V. N. Laukhin, P. A. Kononovich, M. V. Kartsovnik and A. V. Zvarykina: Pis'ma Zh. Eksp. Teor. Fiz. **39** (1984) 275.
9) R. N. Lyubovskaya, R. B. Lyubosvskii, M. K. Makova and S. I. Pesotskii: Pis'ma Zh. Tekh. Fiz. **16** (1990) 80; Fizika (Yugoslavia) **21** Suppl. (1989) 7.
10) L. N. Bulaevskii: Zh. Eksp. Teor. Fiz. **65** (1973) 1278; translation: Sov. Phys. JETP **38** (1974) 634.
11) K. Aoi, W. Dieterich and P. Fulde: Z. Phys. **267** (1974) 223.
12) H. Burkhardt and D. Rainer: Ann. Physik **3** (1994) 181.
13) H. Shimahara: Phys. Rev. B **50** (1994) 12760.
14) H. Shimahara: J. Phys. Soc. Jpn. **66** (1997) 541.
15) L. W. Gruenberg and L. Gunther: Phys. Rev. Lett. **16** (1966) 996
16) A. G. Lebed': Pis'ma Zh. Eksp. Teor. Fiz. **44** (1986) 89; translation: Sov. Phys. JETP Lett. **44** (1986) 144.
17) N. Dupuis: Phys. Rev. B **51** (1995) 9074.
18) G. Yin and K. Maki: Phys. Rev. B **48** (1993) 650.
19) M. Tachiki, S. Takahashi, P. Gegenwart, M. Weiden, M. Lang, C. Geibel, F. Steglich, R. Modler, C. Paulsen and Y. Ōnuki: Z. Phys. B **100** (1996) 369.
20) K. Maki and H. Won: Czech. J. Phys. **46** (1996) Suppl. S2, 1035.
21) S. Matsuo, H. Shimahara and K. Nagai: J. Phys. Soc. Jpn. **64** (1995) 371.
22) H. Shimahara, S. Matsuo and K. Nagai: Phys. Rev. B **53** (1996) 12284.
23) K. Scharnberg and R. A. Klemm: Phys. Rev. B **22** (1980) 5233.
24) E. Helfand and N. R. Werthamer: Phys. Rev. Lett. **13** (1964) 686.
25) I. A. Luk'yanchuk and V. P. Mineev: Zh. Eksp. Teor. Fiz. **93** (1987) 2045; translation: Sov. Phys. JETP **66** (1987) 1168.